



ISSN: 0095-8972 (Print) 1029-0389 (Online) Journal homepage: <http://www.tandfonline.com/loi/gcoo20>

The HNO donor ability of hydroxamic acids upon oxidation with cyanoferrates(III)

María M. Gutiérrez, Alejandra E. Almaraz, Sara E. Bari, José A. Olabe & Valentín T. Amorebieta

To cite this article: María M. Gutiérrez, Alejandra E. Almaraz, Sara E. Bari, José A. Olabe & Valentín T. Amorebieta (2015) The HNO donor ability of hydroxamic acids upon oxidation with cyanoferrates(III), *Journal of Coordination Chemistry*, 68:17-18, 3236-3246, DOI: [10.1080/00958972.2015.1068938](https://doi.org/10.1080/00958972.2015.1068938)

To link to this article: <http://dx.doi.org/10.1080/00958972.2015.1068938>




View supplementary material 



Accepted author version posted online: 24 Jul 2015.
Published online: 31 Jul 2015.



Submit your article to this journal 



Article views: 50



View related articles 



View Crossmark data 

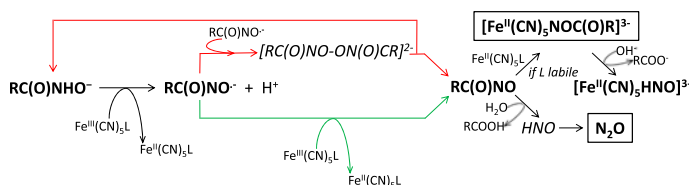
The HNO donor ability of hydroxamic acids upon oxidation with cyanoferrates(III)

MARÍA M. GUTIÉRREZ†, ALEJANDRA E. ALMARAZ†, SARA E. BARI‡, JOSÉ A. OLABE*‡ and VALENTÍN T. AMOREBIETA*†

†Facultad de Ciencias Exactas y Naturales, Departamento de Química, Universidad Nacional de Mar del Plata, Mar del Plata, Argentina

‡Departamento de Química Inorgánica, Analítica y Química Física, INQUIMAE (UBA, CONICET), Buenos Aires, Argentina

(Received 10 April 2015; accepted 10 June 2015)



The hydroxamic acids (RC(O)NHOH, HA) exhibit diverse biological activity, including hypotensive properties associated with formation of nitroxyl (HNO) or nitric oxide (NO). Oxidation of two HAs, benzohydroxamic and acetohydroxamic acids (BHA, AHA) by $[\text{Fe}(\text{CN})_5\text{NH}_3]^{2-}$ or $[\text{Fe}(\text{CN})_6]^{3-}$ was analyzed by spectroscopic, mass spectrometric techniques, and flow EPR measurements. Mixing BHA with both Fe(III) reactants at pH 11 allowed detecting the hydroxamate radical, $(\text{C}_6\text{H}_5\text{C}(\text{O})\text{NO})^\bullet$, as a one-electron oxidation product, as well as N_2O as a final product. Successive UV–vis spectra of mixtures containing $[\text{Fe}(\text{CN})_5\text{NH}_3]^{2-}$ (though not $[\text{Fe}(\text{CN})_6]^{3-}$) at pH 11 and 7 revealed an intermediate acylnitroso-complex, $[\text{Fe}(\text{CN})_5\text{NOC}(\text{O})(\text{C}_6\text{H}_5)]^{3-}$ (λ_{max} , 465 nm, very stable at pH 7), formed through ligand interchange in the initially formed reduction product, $[\text{Fe}(\text{CN})_5\text{NH}_3]^{3-}$, and characterized by FTIR spectra through the stretching vibrations ν_{CN} , ν_{CO} , and ν_{NO} . Free acylnitroso derivatives, formed by alternative reaction paths of the hydroxamate radicals, hydrolyze forming RC(O)OH and HNO, postulated as precursor of N_2O . Minor quantities of NO are formed only with an excess of oxidant. The intermediacy of HNO was confirmed through its identification as $[\text{Fe}(\text{CN})_5(\text{HNO})]^{3-}$ (λ_{max} , 445 nm) as a result of hydrolysis of $[\text{Fe}(\text{CN})_5(\text{NOC}(\text{O})(\text{C}_6\text{H}_5))]^{3-}$ at pH 11. The results demonstrate that hydroxamic acids behave predominantly as HNO donors.

Keywords: Hydroxamic acids; Pentacyano(L)ferrate(III) oxidants; Acylnitroso species; Nitroxyl; Nitroxyl donor

1. Introduction

Hydroxamic acids (RCONHOH, HX) fulfill a variety of physiological roles in biology and medicine, associated with cell signaling, anticancer properties [1], enzyme inhibition [2],

*Corresponding authors. Email: olabe@qi.fcen.uba.ar (J.A. Olabe); amorebie@mdp.edu.ar (V.T. Amorebieta)

and iron-sequestering activities [3, 4]. More recently studied hypotensive abilities are presumably associated with endogenous nitroxyl (HNO, azanone) and NO formation under oxidative stress [5]. In the latter context, HXs are comparatively studied within a group of related compounds like hydroxylamine, hydroxyurea, cyanamide, and azides [6]. Using HXs as therapeutic reagents calls for an investigation of oxidation mechanisms.

It has been well established that HXs can be one-electron oxidized by a wide range of reagents like periodic acid and hexacyanoferrate(III) [7, 8], giving the transient nitroxide radicals, RCONHO^\cdot . The latter species can also be generated from the HXs by pulse- or radiolytically generated OH^\cdot radicals [9]. The fate of the RCONHO^\cdot radicals is not clear [7–9], affording several possible routes, bimolecular radical–radical coupling, as well as other slower unimolecular decompositions, including dismutation (forming HX and the acyl derivative RC(O)N=O , which hydrolyzes to RC(O)OH and HNO), decay to the aldehyde and NO, and homolysis of the C–N bond yielding the acyl radical RC(O)^\cdot and HNO. Mild oxidants like hexacyanoferrate(III) and compound II of heme proteins might also oxidize RCONHO^\cdot to RC(O)N=O . The conditions favoring formation of HNO, NO, or even NO^+ (NO_2^-) during the oxidations of HXs in the biological fluids are a matter of close scrutiny [5, 6].

In the present work, we focus on the oxidative ability of the $[\text{Fe}^{\text{III}}(\text{CN})_5\text{L}]^{n-}$ complexes ($\text{L} = \text{NH}_3, \text{H}_2\text{O}, \text{CN}^-$) [10] toward two selected HA's: acetohydroxamic (AHA) and benzo-hydroxamic (BHA) acids. The series of $[\text{Fe}^{\text{III,II}}(\text{CN})_5\text{L}]^{n,(n+1)-}$ complexes has been widely used in mechanistic studies, particularly in those implying metal- and ligand-based redox processes [10], viz., in the oxidation reactions of hydroxyurea that produce HNO/NO products [11, 12]. We inquired on the possible role of coordination of HX, or of its reaction intermediates/products, at the sites of the $[\text{Fe}^{\text{II}}(\text{CN})_5\text{H}_2\text{O}]^{3-}$ ions. Our contention was based in the contrast expected for the labile $\text{Fe}^{\text{II}}\text{-L}$ bonds in the $[\text{Fe}^{\text{II}}(\text{CN})_5\text{L}]^{3-}$ complexes ($\text{L} = \text{H}_2\text{O}, \text{NH}_3$) compared with the $[\text{Fe}^{\text{II}}(\text{CN})_6]^{4-}$ ion carrying a substitutionally inert $\text{Fe}^{\text{II}}\text{-CN}^-$ bond). The coordination abilities might influence the stoichiometry and mechanism of HX oxidations, and aid identifying reactive intermediates through their distinctive spectral signatures upon coordination.

2. Experimental

$\text{Na}_3[\text{Fe}(\text{CN})_5(\text{NH}_3)] \cdot 3\text{H}_2\text{O}$ and $\text{Na}_2[\text{Fe}(\text{CN})_5(\text{NH}_3)] \cdot \text{H}_2\text{O}$ were prepared and isolated as described in the literature [13, 14]. Solutions of $[\text{Fe}^{\text{III}}(\text{CN})_5\text{L}]^{2-}$ ions ($\text{L} = \text{NH}_3, \text{H}_2\text{O}$) were prepared as recently described [11]. $\text{K}_3[\text{Fe}(\text{CN})_6]$, pyrazinamide, acetohydroxamic, and benzo-hydroxamic acids were purchased from Aldrich. 0.1 M phosphate buffers were used for regulation at pH 7 or 11, with added NaCl to adjust ionic strength up to $I = 1$ M. D_2O and organic solvents (methanol, diethyl ether) were of analytical grade and used without purification. 10^{-3} M EDTA was added in several experiments for complexing the potentially free transition metal (Fe) ions. Argon bubbling was used for the studies in anaerobic conditions.

UV–vis measurements of the reacting solutions, obtained after mixing BHA or AHA with the $\sim 10^{-4}$ M $\text{Fe}(\text{III})$ complexes, were performed under a slight-to-moderate excess of either $[\text{Fe}^{\text{III}}(\text{CN})_5\text{L}]^{2-}$ or HA. A diode array Ocean Optics HE 2000 equipment was used from 200–1100 nm.

IR spectra were measured with a FTIR spectrophotometer, Perkin Elmer Spectrum BX, with a liquid cell containing ZnS windows. The assays were done in H₂O and D₂O solutions, with 7×10^{-2} M [Fe(CN)₅NH₃]²⁻ and 5×10^{-2} M BHA.

The EPR experiments were done with a Bruker ELEXSYS E500 spectrometer. The field was calibrated using a 4 μ M solution of TEMPO ($a_N = 1.72$ mT; $g = 2.0051$) as external standard. The spectra of EPR, at room temperature, were obtained by mixing equal volumes of reactant solutions, buffered and argon-purged, at the desired concentrations. As no radical signals were detected in batch tests, the reaction was performed using a 0.5 cm³ flat flow-cell, and with two-stream fast-mixing, placed in the EPR cavity. The solutions were impulsed to the cell using a continuous flow accessory manually operated. For this setup, the residence time of the reactive solutions in the cell was typically of 0.2–0.3 s [15].

Identification of gaseous products (N₂O, NO) was done with a mass spectrometer Emba II equipped with a thermostated glass reactor and a pressure sensor. N₂O was characterized with m/e 44 and 30 with relative intensities 100 and 30. Quantification was achieved by using a gas manometer, as described elsewhere [11]. The gas evolution was followed by measuring the pressure increase during the reaction process. The eventual formation of nitroprusside in the residual solutions was investigated through its reaction with mercaptosuccinic acid [16]. Stoichiometric experiments of Fe(II) product formation were done by adding a scavenger, like pyrazinamide, to the exhausted solutions and measuring the formation of [Fe^{II}(CN)₅(pyrazinamide)]³⁻ (λ_{\max} , 494 nm, $\epsilon = 4590$ M⁻¹ cm⁻¹) [17]. The results were compared with a control experiment in which ascorbic acid and pyrazinamide were added to the initial [Fe^{III}(CN)₅NH₃]²⁻ reactant, before adding the AH reductant.

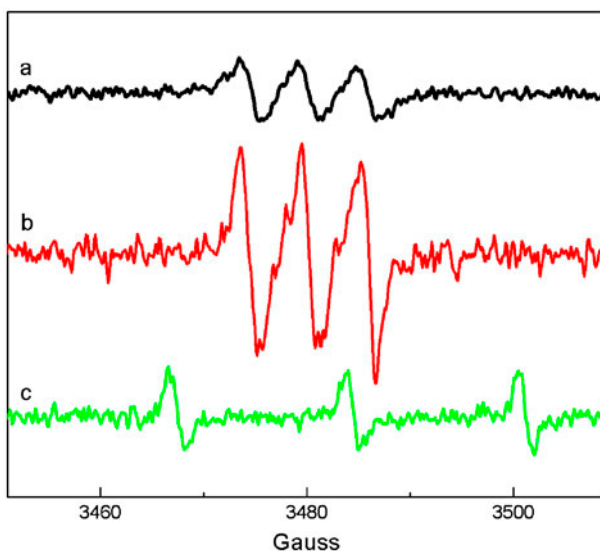


Figure 1. EPR spectra during the reactions of BHA 0.05 M with [Fe^{III}(CN)₅NH₃]²⁻ 0.02 M (a) and [Fe(CN)₆]³⁻ 0.02 M (b), pH 11, 1 M NaCl, 25 °C. The spectrum of TEMPO is shown in (c).

3. Results

3.1. EPR spectra at pH 11

Figure 1 shows the EPR spectrum obtained during the reaction of $[\text{Fe}^{\text{III}}(\text{CN})_5\text{NH}_3]^{2-}$ with BHA. The weak triplet signal, only persistent under flow conditions, may be assigned to the $\text{C}_6\text{H}_5\text{C}(\text{O})\text{NO}^{\bullet-}$ radical ($g_{\text{iso}} = 2.0065$; $a/G = 5.8$). We obtained the same signal by using $[\text{Fe}^{\text{III}}(\text{CN})_6]^{3-}$ as the oxidant, cf. previous observations by Waters [7]. We could not detect any signal with BHA at pH 7 or with AHA (pH 7 or 11).

3.2. Successive UV-vis spectra, pH 11

Figure 2 shows the successive spectra before and after mixing $[\text{Fe}^{\text{III}}(\text{CN})_5\text{NH}_3]^{2-}$ (λ_{max} at 360 and 395 nm) [18] with a 10-fold excess of BHA at 25 °C. Spectrum b (5 min after mixing) already shows the disappearance of the reactant band at 360 nm, though a band at ~400 nm is still maintained. The latter band decays subsequently in a minute time scale, in parallel with a broadening centered at ~450 nm, suggesting the formation of new intermediate species. The final spectrum, several hours after mixing, still shows a broad feature with a main absorption at 400 nm and a shoulder at ~450 nm. Figure SI 1 shows the spectra with AHA under the same conditions, with similar features in the decay of the band at 400 nm compared to figure 2. Figure 3 shows the corresponding display after mixing $[\text{Fe}(\text{CN})_6]^{3-}$ with BHA. The main band of the iron reactant at 415 nm decays in a few seconds, with formation of a product with a weak absorption at ~420 nm. No additional features at greater wavelengths can be observed (cf. with the solutions containing initial $[\text{Fe}^{\text{III}}(\text{CN})_5(\text{NH}_3)]^{2-}$). The decay appears consistent with a previous report on the reaction of $[\text{Fe}(\text{CN})_6]^{3-}$ with $\text{PhCH}_2\text{C}(\text{O})\text{NHOH}$ [7].

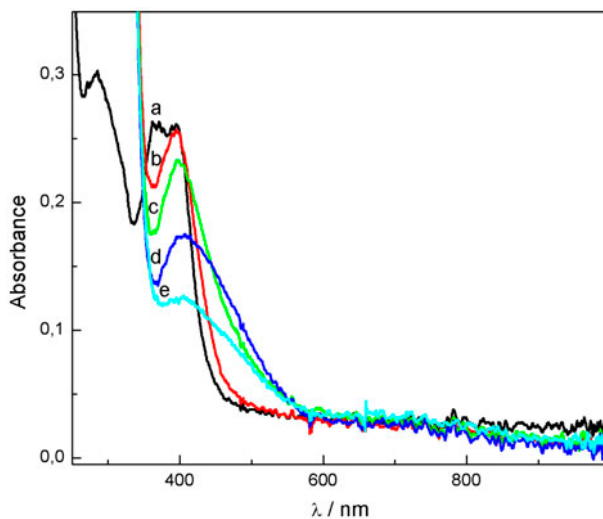


Figure 2. Successive UV-vis spectra for the mixture of $2.5 \times 10^{-4} \text{ M } [\text{Fe}^{\text{III}}(\text{CN})_5\text{NH}_3]^{2-}$ with $2.3 \times 10^{-3} \text{ M}$ BHA, pH 11. Time after mixing, in min: (a) 0, (b) 5, (c) 10, (d) 40 and (e) 360.

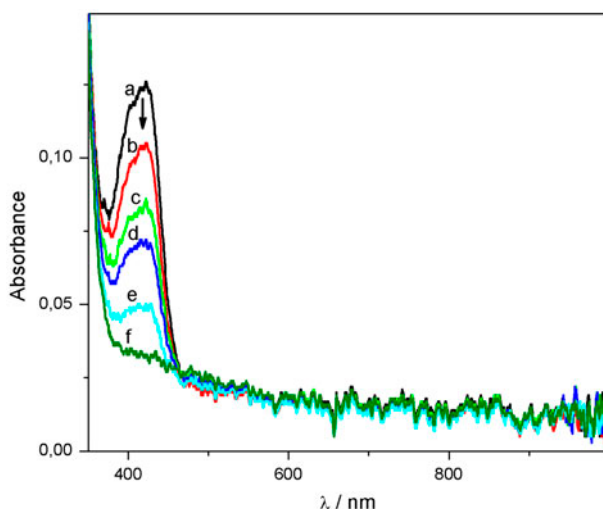


Figure 3. Successive UV-vis spectra for the mixture of 2.5×10^{-4} M $[\text{Fe}^{\text{III}}(\text{CN})_6]^{3-}$ with 2.3×10^{-3} M BHA, pH 11. Time after mixing, in seconds: (a) 0, (b) 0.4, (c) 1.2, (d) 2, (e) 4 and (f) 10.

3.3. Successive UV-vis spectra, pH 7

Figure 4 shows the spectral display showing a similar behavior as previously described in figure 2 at pH 11. The rapid decay of one of the bands of the reactant at 360 nm (cf. spectrum a) can be observed in spectrum b, 10 min after mixing, while the band at ~ 400 nm begins to grow. The successive spectra show the monotonous, slow increase of the latter band absorption, accompanied by a new, more intense band at ~ 460 nm, which attains its maximum intensity in a period of hours.

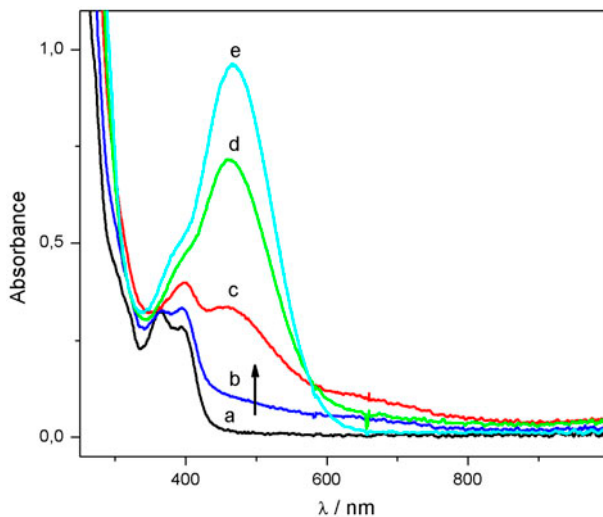


Figure 4. Successive UV-vis spectra for the mixture of 3.9×10^{-4} M $[\text{Fe}^{\text{III}}(\text{CN})_5\text{NH}_3]^{2-}$ with 6.1×10^{-3} M BHA, pH 7. Time after mixing, in min: (a) 0, (b) 10, (c) 20, (d) 35 and (e) 900.

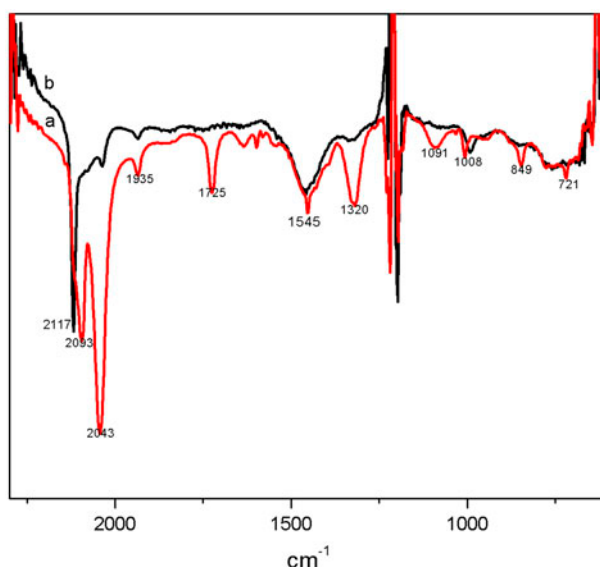


Figure 5. (a) FTIR spectrum in D_2O solution after mixing 7×10^{-2} M $[Fe^{III}(CN)_5NH_3]^{2-}$ with 5×10^{-2} M BHA, 1 M NaCl, 25 °C. (b) Control spectrum with $[Fe^{III}(CN)_5NH_3]^{2-}$.

3.4. FTIR spectra in D_2O

Figure 5 shows the IR spectrum in D_2O , after mixing BHA with $[Fe^{III}(CN)_5NH_3]^{2-}$, at pD of 7-7.5 under a slight excess of the latter complex. It can be seen that decay of the band at 2117 cm^{-1} , corresponding to the Fe(III) species, is accompanied by the onset of new bands at 2093 and 2043 cm^{-1} , typical for values of ν_{CN} in Fe(II) cyano-complexes [10]. A weak band at 1935 cm^{-1} (ν_{NO}) could be assigned to traces of nitroprusside ion [19] $[Fe(CN)_5NO]^{2-}$, originated in the impure Fe(II)/Fe(III) cyano-complexes, or alternatively to additional oxidation of HNO under the slight excess of oxidant. Most significant are the new absorptions at 1725 cm^{-1} (ν_{CO}) [20] and at 1320 cm^{-1} . The latter band may be assigned to ν_{NO} , as also observed in several reduced nitroso-derivatives [21, 22].[†]

3.5. Mass spectral results with gaseous products

The reaction of $[Fe^{III}(CN)_5NH_3]^{2-}$ with BHA and AHA at pH 11 led to exclusive formation of $N_2O(g)$ as a gaseous product. The average yield was lower than 50%, referred to the initial moles of nitrogen in AHA or BHA. With AHA, the reaction at pH 7 also generated minor quantities of $NO(g)$. This could arise through a competitive path for the hydroxamate decomposition, namely the disproportionation to NO and $RCHO$ [5(c)].

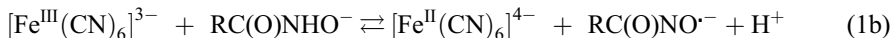
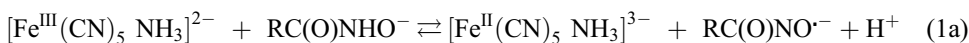
[†]Values of ν_{NO} in the range $1300\text{--}1400\text{ cm}^{-1}$ indicate that the nitrosyl group is in a reduced state, comprising a bond order close to 2, and this is observed for many members of the series $[Fe^{II}(CN)_5NOX]^{n-}$, with X = thiolates, H, alkyls, etc. [22].

3.6. Stoichiometric experiments of iron redox conversion

In the reaction of $[\text{Fe}^{\text{III}}(\text{CN})_5\text{NH}_3]^{2-}$ with a slight excess of AHA or BHA, we observed ~ 1.5 equivalent consumption ratio ($[\text{Fe}^{\text{III}}]/[\text{HA}]$), either by performing experiments with or without EDTA, both at pH 7 and 11. In the experiments using $[\text{Fe}^{\text{III}}(\text{CN})_6]^{3-}$ as the oxidant, we found the same 1.5 stoichiometry in the absence of EDTA, though a change to a 1 : 1 stoichiometry if EDTA was added (as also found by Waters [7]). The greater consumption of oxidant (associated to a fast process leading to a 1 : 1 ratio followed by a slower process involving ~ 0.5 additional equivalents) has been assigned to reordering of the initially formed hydroxamate radicals [7].

4. Discussion

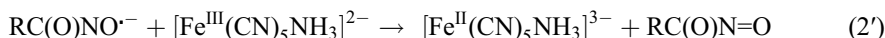
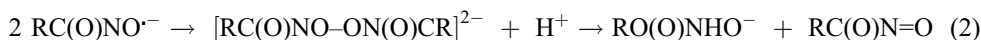
The EPR results after mixing $[\text{Fe}^{\text{III}}(\text{CN})_5\text{L}]^{n-}$ ($\text{L} = \text{NH}_3, \text{CN}^-$) with BHA at pH 11 (figure 1) allow proposing reactions (1a and 1b) as the first rapid steps (second-time scale) comprising a one-electron oxidation of the hydroxamate anion $\text{C}_6\text{H}_5\text{C}(\text{O})\text{NHO}^-$ (pK_a of HA's = ~ 9) [5, 9]. The inability to detect any radicals for BHA at pH 7 is probably associated with the greater reactivity of the protonated radical species.



Reaction (1a) involves the reduction of $[\text{Fe}^{\text{III}}(\text{CN})_5\text{NH}_3]^{2-}$ to $[\text{Fe}^{\text{II}}(\text{CN})_5\text{NH}_3]^{3-}$, as indicated in figure 2 by the onset of a residual band at ~ 400 nm, typical of the Fe(II) species [10]. We assume that similar radicals are also formed with AHA, given the common reactivity pattern described in the Results section. Figure SI 1 indicates the UV-vis spectral evolution for AHA. Fast initial steps like (1) have also been reported previously for other HA's [7].

The corresponding EPR spectrum in figure 1 displays the oxidative activity of $[\text{Fe}^{\text{III}}(\text{CN})_6]^{3-}$, also occurring rapidly, comparable with $[\text{Fe}^{\text{III}}(\text{CN})_5\text{NH}_3]^{2-}$. Figure 3 shows the spectral evolution found for $[\text{Fe}^{\text{III}}(\text{CN})_6]^{3-}$ with a product identified as $[\text{Fe}^{\text{II}}(\text{CN})_6]^{4-}$ (spin-forbidden band at 422 nm) [23], (reaction 1b). Given the comparable redox potentials (~ 0.4 V) for the $[\text{Fe}^{\text{III}}(\text{CN})_5\text{NH}_3]^{2-}/[\text{Fe}^{\text{II}}(\text{CN})_5\text{NH}_3]^{3-}$ and $[\text{Fe}^{\text{III}}(\text{CN})_6]^{3-}/[\text{Fe}^{\text{II}}(\text{CN})_6]^{4-}$ redox couples [10], the similar rates for the initial step obtained for both oxidants toward AHs become fully consistent.

In general, the radicals formed in the one-electron oxidations ($\text{pK}_a \sim 9$) show complex subsequent reactivity [7, 9], suggesting fast recombination processes ($k \sim 10^7 \text{ M}^{-1} \text{ s}^{-1}$) [9]. The spin density at the O-C-N-O group allows generating diverse adducts (C-C, N-N, C-O, N-O, O-O) as a result of alternative couplings of the different isomers of the nitroxide radical [5(c)]. The results show that the very reactive O-O adduct (derived from the RC(O)NO $^{\cdot-}$ isomer) dismutates yielding the parent X $^-$ and an acyl-nitroso species, as described in reaction (2). The latter compound could be generated through the alternative reaction pathway (2') [9].



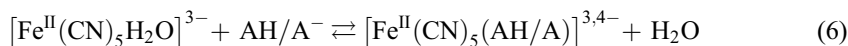
The formation of an intermediate acyl-nitroso species has been considered as crucial for hydrolytic generation of nitroxyl, HNO/NO^- (reaction (3)), when the solutions of hydroxyurea and related species react with oxidants [20]. HNO might be trapped by available acceptors in the medium, in competition with its rapid dehydrative dimerization giving N_2O , reaction (4), with $k = 8 \times 10^6 \text{ M}^{-1} \text{ s}^{-1}$ [24].



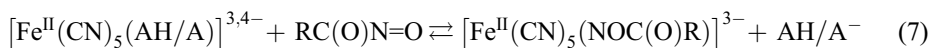
$[\text{Fe}^{\text{II}}(\text{CN})_5\text{NH}_3]^{3-}$ is susceptible to aquation, as described in reaction (5), with a half-life of 40 s for release of NH_3 at 25 °C [25]. At pH 7, reaction (5) is completely displaced by protonation of NH_3 , and therefore the $[\text{Fe}^{\text{II}}(\text{CN})_5\text{H}_2\text{O}]^{3-}$ ion will be quantitatively generated in a few minutes. At pH 11, however, an equilibrium is established, with persistence of $[\text{Fe}^{\text{II}}(\text{CN})_5\text{NH}_3]^{3-}$ [26, 27].[†]



Under excess AH/A^- , N-binding to the labile aqua-site might occur through reaction (6), as suggested by the persistence of the 400 nm band:



However, $[\text{Fe}^{\text{II}}(\text{CN})_5(\text{AH/A})]^{3,4-}$ is expected to be sufficiently labile toward dissociation (like $[\text{Fe}^{\text{II}}(\text{CN})_5\text{NH}_3]^{3-}$) and can lead to reaction (7) through a ligand interchange reaction with the acyl-nitroso group formed in (2) or (2').



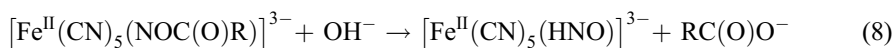
We assign the intense bands observed at 465 nm (pH 7) during the slow reactions occurring subsequently to the initial reduction (both with BHA and AHA, figures 4 and SI 1) to the corresponding products in reaction (7). We rely on the close similarity with the well-established coordination ability of nitrosoalkanes $[\text{Fe}^{\text{II}}(\text{CN})_5 \text{N(O)CH}_2\text{C}(\text{CH}_3)_2\text{OH}]^{3-}$ [28] and nitrosoformamide $[\text{Fe}^{\text{II}}(\text{CN})_5\text{NOC(O)NH}_2]^{3-}$ [11]. The latter compound was isolated as a sodium salt, after oxidation of hydroxyurea with cyanoferrates(III), in a

[†]Transient absorptions in the visible region (cf. figure 3), and the rising weak absorptions at ~1000 nm can be assigned to cyano-bridged dinuclear species containing $[\text{Fe}^{\text{III}}, \text{Fe}^{\text{III}}]$ and $[\text{Fe}^{\text{II}}, \text{Fe}^{\text{III}}]$ chromophores. They are generated under the initial oxidative conditions (associated with Fe(III) concentrations greater than $\sim 10^{-4} \text{ M}$) and decay in a dissociative way under an excess of AH [23, 24].

reaction closely similar to the one reported here. All of these compounds show intense charge-transfer bands at ~ 460 nm, as well as consistent signatures in the IR spectra corresponding to the ν_{NO} , ν_{CO} , and ν_{CN} stretching frequencies, as shown by the presently reported intermediate (see figure 5, Results section).

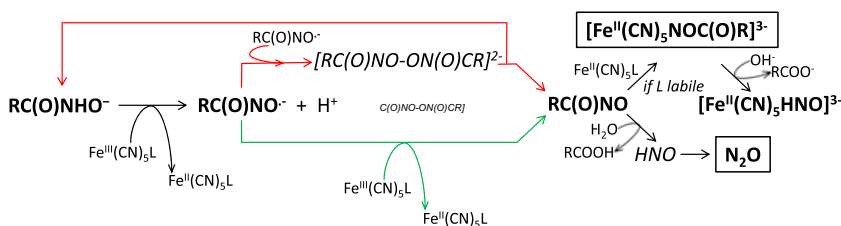
For reaction (7), the maximum absorbance value obtained at 465 nm (figure 4) suggests that less than a 50% yield of $[\text{Fe}^{\text{II}}(\text{CN})_5(\text{NOC}(\text{O})\text{R})]^{3-}$ is obtained, with respect to the total iron content (we estimate a molar absorptivity of $\sim 4 \times 10^3 \text{ M}^{-1} \text{ cm}^{-1}$ for $[\text{Fe}^{\text{II}}(\text{CN})_5(\text{NOC}(\text{O})\text{R})]^{3-}$) [11]. This is due, on the one hand, to the additional, unidentified products of radical reactions [9]. On the other hand, free $\text{RC}(\text{O})\text{N}=\text{O}$ may decompose via hydrolysis (catalyzed by OH^-), yielding HNO [21, 29], which would rapidly lead to N_2O release (equations (3) and (4)). The yields of N_2O , generally less than 50% (see Results), are consistent with the above explanation.

Remarkably, $[\text{Fe}^{\text{II}}(\text{CN})_5(\text{NOC}(\text{O})\text{R})]^{3-}$ is strongly stabilized at pH 7, though not at pH 11, given that only shoulders are apparent at 465 nm in the latter case (figures 2 and SI 1 for BHA and AHA, respectively). This is consistent with the hydrolysis of the bound acyl-nitroso group to HNO occurring more favorably at pH 11 [29], as described in reaction (8).



Strong evidence for reaction (8) is apparent from the broadening of the band in the aged spectra, compatible with the distinctive maxima for the reactant and the product at 465 and 445 nm, respectively. The spectroscopic and kinetic properties of the $[\text{Fe}^{\text{II}}(\text{CN})_5(\text{HNO})]^{3-}$ ion have been recently described, showing an intense charge-transfer band at 445 nm [30, 31]. Reaction (8) provides good supporting evidence on the successive formation of acyl-nitroso \rightarrow nitroxyl species as necessary precursors of N_2O release.

Scheme 1 describes the proposed mechanism. It can be concluded that hydroxamic acids behave mainly as HNO donors after mixing with the cyanoferrates(III), once the $\text{N}(+1)$ redox state has been reached by forming the $\text{RC}(\text{O})\text{N}=\text{O}$ intermediate, as recently proposed for other strong oxidants like OH^\cdot radicals, as well as milder oxidants like compounds I or II arising in the mixtures of heme-proteins and H_2O_2 [5(c)]. At both pH 7 and 11, the successive UV-vis spectra (when using $[\text{Fe}^{\text{III}}(\text{CN})_5\text{NH}_3]^{2-}$) demonstrate that the HAs may bind to $\text{Fe}(\text{II})$ complexes generated upon fast initial reduction of $\text{Fe}(\text{III})$ complexes, followed by successive conversions to the acyl-nitroso species, which in turn may lead to HNO ligand. We also observed some minor NO when an excess of oxidant was used. There is a thermodynamic ability of cyanoferrates(III) for oxidizing bound HNO to NO/NO^+ , as recently demonstrated by oxidation of the nitroxyl complex $[\text{Fe}^{\text{II}}(\text{CN})_5(\text{HNO})]^{3-}$ up to



Scheme 1. Reaction mechanism.

nitroprusside after addition of $[\text{Fe}^{\text{III}}(\text{CN})_6]^{3-}$ [31]. With respect to the influence of coordination on the mechanistic aspects of hydroxamate reactivity, the results show that N_2O is always formed for every L, and that no significant changes in the rates for the initial redox step are observed when $[\text{Fe}^{\text{III}}(\text{CN})_6]^{3-}$ is replaced by $[\text{Fe}^{\text{III}}(\text{CN})_5(\text{NH}_3)]^{2-}$ or $[\text{Fe}^{\text{III}}(\text{CN})_5(\text{H}_2\text{O})]^{2-}$. The fact that $[\text{Fe}^{\text{III}}(\text{CN})_6]^{3-}$ is still a source of N_2O (in spite of the substitution-inert $\text{Fe}^{\text{III}}\text{--C}$ and $\text{Fe}^{\text{II}}\text{--C}$ bonds) indicates that the coordination step is not crucial for HNO formation. Instead, HNO, and subsequently N_2O , form mainly through the hydrolysis of *free* acyl-nitroso, which in turn is generated by a one-electron oxidation of the hydroxamate radical. For all the studied complexes, HNO generated in this way may react with potential biological targets such as thiols and metalloproteins under competition with the dehydrative dimerization leading to N_2O . In addition, it can be converted to NO under an oxidizing environment. We conclude that the labile Fe(II)-aqua coordination site allows binding and identifying the HX, $\text{RC}(\text{O})\text{N}=\text{O}$, and HNO intermediates, though clearly the main route to HNO and N_2O formation does not depend on the competitively formed bound species. In fact, the $[\text{Fe}^{\text{II}}(\text{CN})_5(\text{RC}(\text{O})\text{N}=\text{O})]^{3-}$ ion appears to be very robust toward hydrolysis at pH 7. On the other hand, HNO dissociates very slowly from $[\text{Fe}^{\text{II}}(\text{CN})_5(\text{HNO})]^{3-}$, precluding N_2O formation [31].

Acknowledgements

We thank the Universities of Mar del Plata and Buenos Aires for support. This work benefited from grants of CONICET and the University of Buenos Aires. SEB, JAO, and VTA are members of the research staff of CONICET.

Disclosure statement

No potential conflict of interest was reported by the authors.

Funding

This work was supported by the Consejo Nacional de Investigaciones Científicas y Técnicas [grant number PIP 112–200801–02817]; Universidad de Buenos Aires [grant number 01/W391].

Supplemental data

Supplemental data for this article can be accessed here [<http://dx.doi.org/10.1080/00958972.2015.1068938>].

References

- [1] P. Kovacic, C.L. Edwards. *J. Recept. Signal Transduct. Res.*, **31**, 10 (2011).
- [2] C.J. Marmion, D. Griffith, K.B. Nolan. *Eur. J. Inorg. Chem.*, **15**, 3003 (2004).
- [3] R. Codd. *Coord. Chem. Rev.*, **252**, 1387 (2008).
- [4] N. Gálvez, B. Ruiz, R. Cuesta, E. Colacio, J.M. Domínguez-Vera. *Inorg. Chem.*, **44**, 2706 (2005).

- [5] (a) Y. Samuni, U. Samuni, S. Goldstein. *Biochim. Biophys. Acta*, **1820**, 1560 (2012); (b) Y. Samuni, D.A. Wink, M.C. Krishna, J.B. Mitchell, S. Goldstein. *Free Radical Biol. Med.*, **73**, 291 (2014); (c) S. Goldstein, A. Samuni. *Adv. Inorg. Chem.*, **67**, 315 (2015).
- [6] J.A. Reisz, E. Bechtold, S.B. King. *Dalton Trans.*, **39**, 5203 (2010).
- [7] (a) T.R. Oliver, W.A. Waters. *J. Chem. Soc. (B)*, 677 (1971); (b) D.F. Minor, W.A. Waters, J.K. Ramsbottom. *J. Chem. Soc. (B)*, 180 (1967).
- [8] J.M. Leal, B. Garcia, P.L. Domingo. *Coord. Chem. Rev.*, **173**, 79 (1998).
- [9] A. Samuni, S. Goldstein. *J. Phys. Chem.*, **115**, 3022 (2011).
- [10] (a) J.A. Olabe. *Adv. Inorg. Chem.*, **55**, 61 (2004); (b) J.A. Olabe. *Dalton Trans.*, **28**, 3633 (2008).
- [11] A.C. Montenegro, S.G. Dabrowski, M.M. Gutiérrez, V.T. Amorebieta, S.E. Bari, J.A. Olabe. *Inorg. Chim. Acta*, **374**, 447 (2011).
- [12] A. Budimir, E. Besic, M. Birus. *Croat. Chem. Acta*, **82**, 807 (2009).
- [13] D.J. Kenney, T.P. Flynn, J.B. Gallini. *J. Inorg. Nucl. Chem.*, **20**, 75 (1961).
- [14] G. Brauer. *Handbook of Preparative Inorganic Chemistry*, 2nd Edn, Academic Press, New York (1965).
- [15] M.M. Gutiérrez, G.B. Alluisetti, C. Gaviglio, F.A. Doctorovich, J.A. Olabe, V.T. Amorebieta. *Dalton Trans.*, 1187 (2009).
- [16] F. Roncaroli, J.A. Olabe, R. van Eldik. *Inorg. Chem.*, **41**, 5417 (2002).
- [17] P.J. Morando, V.I.E. Bruyere, M.A. Blesa, J.A. Olabe. *Transition Met. Chem.*, **8**, 99 (1983).
- [18] A.R. Parise, S. Pollak, L.D. Slep, J.A. Olabe. *Anales Asoc. Qca. Arg.*, **83**, 211 (1995).
- [19] J.D. Schwane, M.T. Ashby. *J. Am. Chem. Soc.*, **124**, 6822 (2002).
- [20] A.D. Cohen, B.B. Zeng, S.B. King, J.P. Toscano. *J. Am. Chem. Soc.*, **125**, 1444 (2003).
- [21] S.B. King. *Curr. Top. Med. Chem.*, **5**, 665 (2005).
- [22] S.E. Bari, J.A. Olabe, L.D. Slep. *Adv. Inorg. Chem.*, **67**, 87 (2015).
- [23] H.B. Gray, N.A. Beach. *J. Am. Chem. Soc.*, **85**, 2922 (1963).
- [24] V. Shafirovich, S.V. Lyman. *Proc. Natl. Acad. Sci. U.S.A.*, **99**, 7340 (2002).
- [25] (a) H.E. Toma. *Inorg. Chim. Acta*, **15**, 205 (1975); (b) H.E. Toma, J.M. Malin. *Inorg. Chem.*, **12**, 1039 (1973).
- [26] A.D. James, R.S. Murray, W.C.E. Higginson. *J. Chem. Soc., Dalton Trans.*, 1273 (1974).
- [27] M.F. Souto, F.D. Cukiernik, P. Forlano, J.A. Olabe. *J. Coord. Chem.*, **54**, 343 (2001).
- [28] R.P. Cheney, M.G. Simic, M.Z. Hoffman, I.A. Taub, K.D. Asmus. *Inorg. Chem.*, **16**, 2187 (1977).
- [29] X. Sha, T.S. Isbell, R.P. Patel, C.S. Day, S.B. King. *J. Am. Chem. Soc.*, **128**, 9687 (2006).
- [30] A.C. Montenegro, V.T. Amorebieta, L.D. Slep, D.F. Martín, F. Roncaroli, D.H. Murgida, S.E. Bari, J.A. Olabe. *Angew. Chem. Int. Ed.*, **48**, 4213 (2009).
- [31] A.C. Montenegro, S.E. Bari, J.A. Olabe. *J. Inorg. Biochem.*, **118**, 108 (2013).